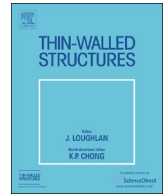




ELSEVIER

Contents lists available at ScienceDirect

Thin-Walled Structures

journal homepage: www.elsevier.com/locate/tws

Full length article

Artificial neural networks and intelligent finite elements in non-linear structural mechanics

Marcus Stoffel*, Franz Bamer, Bernd Markert

Institute of General Mechanics, RWTH Aachen University, Templergraben 64, D-52056 Aachen, Germany

ARTICLE INFO

MSC:
74K20
74-05

Keywords:

Artificial neural network
Structural mechanics
Intelligent finite element

ABSTRACT

In recent years, artificial neural networks were included in the prediction of deformations of structural elements, such as pipes or tensile specimens. Following this method, classical mechanical calculations were replaced by a set of matrix multiplications by means of artificial intelligence. This was also continued in finite element approaches, wherein constitutive equations were substituted by an artificial neural network (ANN). However, little is known about predicting complex non-linear structural deformations with artificial intelligence. The aim of the present study is to make ANN accessible to complicated structural deformations. Here, shock-wave loaded plates are chosen, which lead to a boundary value problem taking geometrical and physical non-linearities into account. A wide range of strain-rates and highly dynamic deformations are covered in this type of deformation. One ANN is proposed for the entire structural model and another ANN is developed for replacing viscoplastic constitutive equations, integrated into a finite element code, leading to an intelligent finite element. All calculated results are verified by experiments with a shock tube and short-time measurement techniques.

1. Introduction

Artificial neural networks have been applied in engineering problems as an alternative approach compared to classical methods based on continuum mechanical modelling. Promising results were achieved by investigating stress-strain curves of metal specimens under high-temperature [1], design of steel structures [2], vibrations of structures [3,4], or stability problems of structures [5]. Reliability studies of structures were reported in [6] and influences of welding on material properties are investigated in [7]. An ANN can lead to much lower computational time and can replace the mechanical model completely. It can be trained by experimental data, only, and needs therefore no identification of material parameters. Consequently, a mathematical model is generated by means of an algebraic system of equations. Following this approach, the ANN approximates to the trained data. The learning procedure of the ANN is based on the examples, which are provided by the user [8]. However, weaknesses of ANNs have been reported in [9] due to the difficulties of interpreting parameters in neural networks, e.g. the number of hidden layers or neurons. Also the components of the synapse matrices of a trained ANN can hardly be interpreted as it can be done with material parameters in a constitutive law. In several studies, the problem of a so-called black box is described [10,11]. Consequently, it is difficult to find reasons to explain discrepancies between predictions using ANN and experimental data.

Once, the ANN has been trained well with input and output data sets, it can recalculate the provided data very accurately. However, predictions beyond that data can lead to uncertain results, which is documented in literature [12]. An additional approach using the advantages of ANN together with well-established numerical methods is the development of intelligent finite elements. These elements have been proposed in literature, leading to a combination of classical finite elements with an ANN and are used only for a part of the entire mechanical model. Studies substituting the constitutive model by means of an ANN have been published in [13]. A beam element, based on a neural network, is proposed in [14] and leads to lower computational costs than a classical approach. This benefit is even more pronounced since multiscale approaches are concerned [15]. In literature several neural network constitutive models (NNCM) were discussed [16]. However, it was reported that the choice of the provided training data is essential for a reliable intelligent finite element [17].

The substitution of nonlinear structural and material models for two-dimensional structures by ANNs is, to the knowledge of the authors, not yet well known in literature. Structures, such as plates and shells, are widely used in engineering, can be subjected to dynamic loadings and can undergo geometrically non-linear deformations with inelastic strains. Especially, the correct modelling of strain-rate dependency of structural deformations is subject of current research [18–20]. In the present study, metal plates are loaded impulsively by

* Corresponding author.

E-mail address: stoffel@iam.rwth-aachen.de (M. Stoffel).

shock waves causing viscoplastic deformations and high inelastic strain rates. The aim is to propose an ANN, which is able to predict these highly non-linear structural deformations. The ANN is developed in two ways. Firstly, a neural network is proposed, trained by experimental data only and, afterwards, it is used to predict structural deformations in additional experiments. Secondly, in order to overcome discrepancies between measurements and calculations, an intelligent finite element is proposed, wherein the constitutive equations are replaced by an ANN. This neural network is trained with data about stresses, strains, strainrates and hardening in a range, which is expected in the finite element simulations. Following this strategy, we exploit the advantage of ANNs to be very accurate since only trained data is used. The intelligent finite element is implemented in a code for a geometrically non-linear first-order shear deformation shell theory. In this way, a classical shell theory is combined with an ANN substituting a physically nonlinear constitutive law and leading to low simulation times. By means of the proposed method, ANNs shall be accessible to nonlinear structural problems in engineering.

2. Experiment

The measured results of structural deformations are obtained by experiments in a shock tube, see [21]. In Fig. 1, the used set-up of the shock tube is shown, consisting of a high (HPC) and a low pressure chamber (LPC), separated from each other by an aluminum membrane. After an increase of the gas pressure in the HPC, the membrane is destroyed, causing a shock wave, which propagates the shock tube towards the aluminum plate specimen in the LPC. If the shock wave hits the plate, then a high-pressure and high-density impulse is caused on the specimen leading to viscoplastic deformations in time scales of several microseconds.

The mid-point displacement of the circular specimen and the pressure acting on the plate during the time are measured by means of short-time measurement techniques. The experiments are carried out with different thicknesses of membranes between the HPC and LPC and with different gases in the HPC, such as nitrogen and helium. In this way, different pressure peaks (pp) and pressure evolutions can be caused on the specimen. The plate specimens are 2 mm thick and exhibit a diameter of 553 mm. In Fig. 2, four experiments with mid-point displacements (Dis.) of the plates and pressures (Pre.) acting on them are presented. Three of them will be used to train the ANN and the fourth one is taken as a reference for the validation of the ANN. The measurements can be recorded down to 1 μs sample rate in order to assure that enough experimental data is available to train the ANN. The capacitive displacement sensor, developed in [21] and the piezoelectric pressure sensors exhibit an inertia small enough to record fast signal changes.

3. Artificial neural network for the entire structure

The ANN developed in this study is based on a feed forward network, which is well established in literature [22]. The present

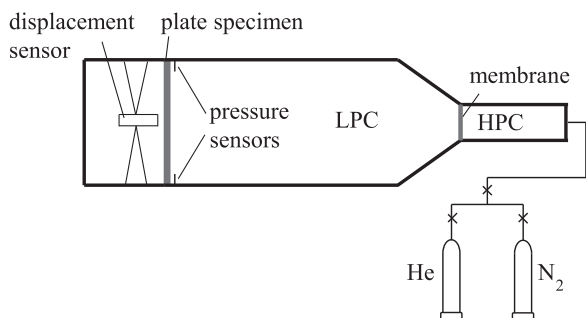


Fig. 1. Principle of the shock tube.

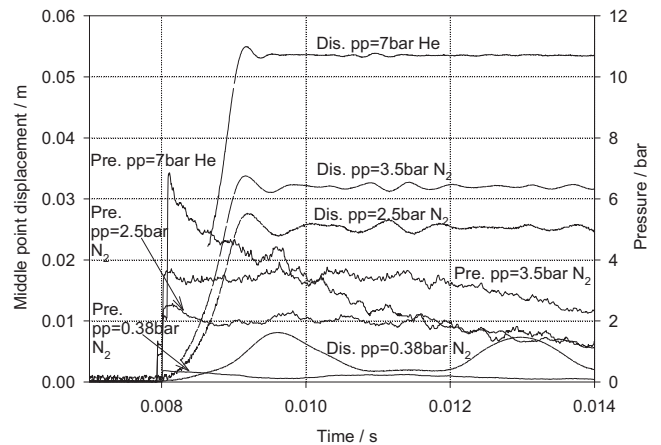


Fig. 2. Plate deflections under high speed pressure loadings with peak pressures (pp) at the specimen and helium and nitrogen in the HPC.

algorithm consists of three layers and is implemented in python. The input layer includes three neurons, representing time, pressure, and shock wave propagation velocity. The hidden layer is composed of eight neurons and the output layer has one neuron denoting the mid-point displacement of the plate specimen. In incremental approaches, as in the finite element method, increments of state variables, e.g. strains and displacements, are accumulated during the simulation. However, in the present study, the ANN uses ordered pairs of values with the mentioned input and output values, i.e. one pressure, one mid-point displacement, and one propagation velocity can exist only at one instance of time. If we ignored one of these neurons, then ambiguous solutions would be possible. For this reason, the time is treated as a state variable in the ANN as e.g. the mid-point displacement.

In Fig. 3, the architecture of the ANN is shown. In order to optimize the least square error between calculated output and provided output data, a gradient descent algorithm in form of the back propagation method is applied. All values used in the ANN are normalised due to better convergence [1,23]. In [24], it was described that it is necessary to obtain numerical stability with homogeneous values. Here, this is carried out for input and output values x_i by

$$X_i = 0.1 + 0.8 \cdot \left(\frac{x_i - x_{min}}{x_{max} - x_{min}} \right)$$

leading to unified values X_i and with x_{min} and x_{max} as minimum and maximum values of each input and output value, respectively. The propagation function includes the weights w_{ij} , which exhibit random values initially. They represent the weights of the connections between

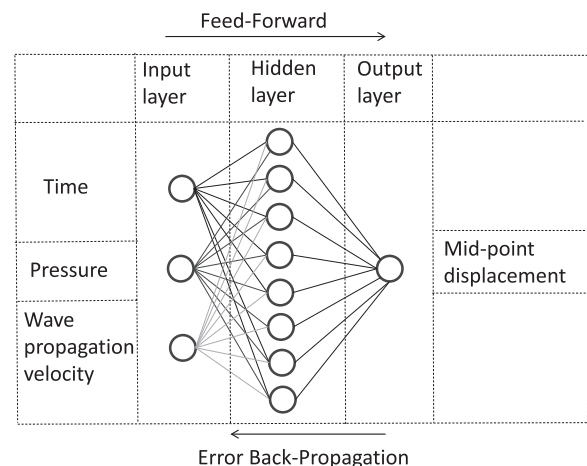


Fig. 3. Artificial neural network for the entire structure.

the neurons. During the training procedure the weights are determined iteratively and the products of input signals together with the weights are added in the propagation function

$$p_j = \sum_{i=1}^n X_i w_{ij}$$

with n as the number of inputs. Here, p_j is the sum of all input values X_i multiplied with the weights w_{ij} for the j -th neuron in the next layer. Due to three layers in the ANN, two weight matrices will be obtained. The system of matrices denote an algebraic set of equations. In order to generate an output signal, an activation function is necessary, which is monotonically increasing. The function F_j determines for one neuron j the output signal. Here, from a variety of possible activation functions, the sigmoid function is chosen:

$$F_j = \frac{1}{1 + e^{-p_j}}$$

For more detailed information about activation and propagation functions with the considered weights, it is referred to textbooks such as [25].

The function approximation by means of ANNs can be mathematically nonconstructive. Consequently, this effect leads to the problem, that internal variables of the ANN, e.g the number of hidden layers, have to be proposed by the user. Analogously, the same procedure is applied to the determination of the number of weights and, if necessary, biases between the layers [15,26]. These quantities have to be defined by an iterative process, based on an optimum criterion. For this reason, here, the smallest mean square error between the predicted values and the experimentally obtained output values was used to identify the number of neurons in the hidden layer. After training with experimental data, the ANN can very precisely recalculate the measured output values. However, it is documented in literature that even well-trained ANNs can cause inaccurate results, if the input data differs from the trained set of values [9,11,12]. In the present investigation in this section, the accuracy of the extrapolated data is studied.

In Fig. 4, results of the trained and verified ANN in normalised format are presented. In this diagram, three mid-point displacements of the output neuron are connected with each other, denoting the amount of data points used to train the ANN. For the trained model altogether 1200 input and output data points were used. A good correlation of the trained ANN with the experimental data can be observed. However, regarding the validation with a fourth experiment, the correlation of the predicted output is not as good as in the trained case. Similar results are obtained, if trained and validated output values are exchanged. However, the mid-point deflection, which was used in Fig. 4 for validation, is shown in Fig. 5 for another calculation with physical values after training.

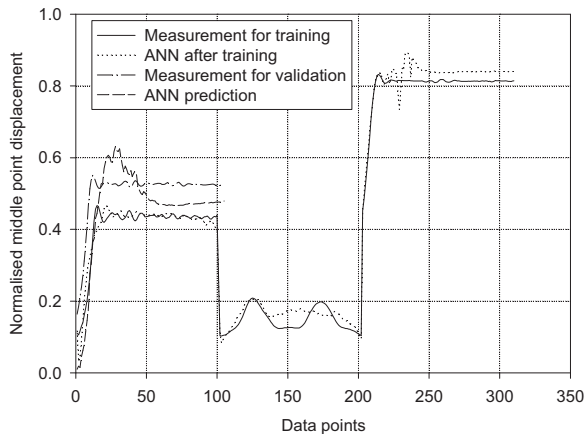


Fig. 4. Normalised mid-point displacements after training and validation.

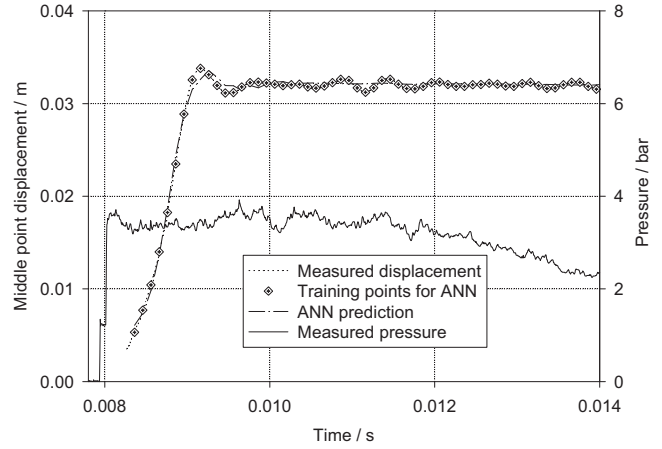


Fig. 5. ANN simulation, FEM simulation and measurement of mid-point displacements during shock-wave loading.

Here, only several training points are provided for the ANN and the prediction of the mid-point deflections is very close to the measurement. Consequently, the ANN can recalculate the given data sets during the training, as shown in Fig. 4, very accurately. Weaknesses in predictions occur, if the ANN has to inter- or extrapolate with new input data. For this reason, in the next sections, an intelligent finite element is proposed, which uses only data of a trained ANN.

4. Non-linear structural and material model

In [21], a geometrically and physically nonlinear shell model, taking first-order shear deformations into account, was used. Due to the combination of a structural model with viscoplastic constitutive equations, developed in [27], it was possible to account for strain-rate dependency. In previous works, an extensive effort was made to identify material parameters. In the present work, this step is not necessary anymore, because the following constitutive relations are replaced by an intelligent element:

$$\varepsilon_{ij}^{\dot{p}} = \frac{3}{2} \dot{p} \frac{\sigma'_{ij} - X'_{ij}}{J_2(\sigma'_{rs} - X'_{rs})}, \quad (1)$$

$$\dot{p} = \left\langle \frac{\sigma_v}{K} \right\rangle^n, \quad (2)$$

$$\sigma_v = J_2(\sigma'_{ij} - X'_{ij}) - R - k, \quad (3)$$

$$\dot{X}_{ij} = \frac{2}{3} a \dot{\varepsilon}_{ij}^p - s X_{ij} \dot{p}, \quad \dot{R} = b_1(b_2 - R) \dot{p}. \quad (4)$$

Here, $\varepsilon_{ij}^{\dot{p}}$, σ_{ij} , X_{ij} , R , k , p , σ_v denote plastic strain tensor, stress tensor, backstress tensor, isotropic hardening, yield limit, equivalent plastic strain, overstress, and a , s , b_1 , b_2 , n , K are material parameters. The deviatoric part of a tensor is denoted by $(\cdot)'$, $\dot{(\cdot)}$ indicates the material time derivative. All plate and tensile specimens are cut out of thin metal sheet plates. For this reason, cyclic material tests to separate kinematic and isotropic hardening from each other are not possible. Consequently, pure kinematic hardening was assumed. Based on this strongly nonlinear model, finite element simulations were carried out in previous works, which are used in this study as an additional validation result together with the measurements. Due to the structural assumption of a constant shell thickness during deformations, the stress, strain, and backstress tensors include only five components, two in the direction of the midsurface and three shear components.

5. Intelligent finite element

In the intelligent finite element, the viscoplastic material law, used

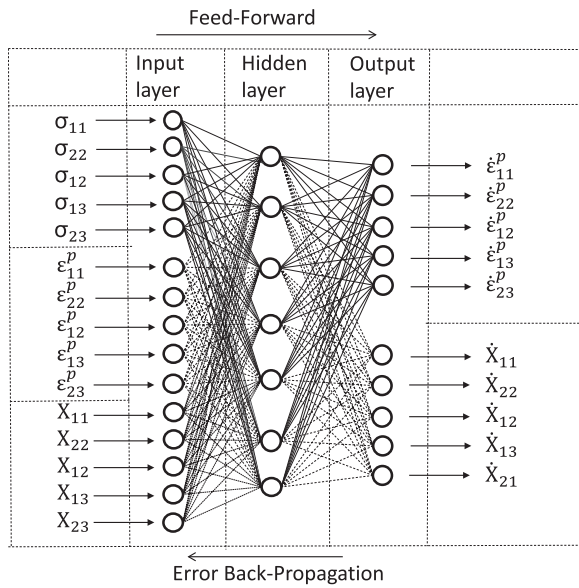


Fig. 6. Artificial neural network for a viscoplastic material model.

in the Gaussian quadrature points, is substituted by a trained ANN. The data to train the model is obtained by numerical simulations with the finite element code, described in the cited previous studies. A set of constitutive data is generated with five stress, backstress, and plastic strain tensor components for the input layer. The output layer consists of five plastic strainrate and backstressrate tensor components. The neural network, shown in Fig. 6 with three layers, 15 neurons in the input layer, seven neurons in the hidden layer and ten neurons in the output layer, is proposed.

This ANN is trained with 1500 input and output data points in order to obtain two synapse matrices including the weights, see Eq. (3). From previous studies, it was ensured that the state variables, occurring in the simulations with an ANN, will be in the range of the trained data. E.g. normal stresses are in-between 1.5 N/mm² and -1 N/mm². All state variables are normalised as presented in Eq. (3).

For the training of the ANN the same python code is used as described in Section 3, leading to the determination of the two synapse matrices. Afterwards, the viscoplastic constitutive equations in the finite element code are replaced by the ANN. During the calculations, all input variables were normalised and the output variables were determined by the ANN integrated into the finite element code. The normalised output variables were transformed back to physical values. In this way, the simulations are using only trained ANN data. However, small interpolations between trained data points are possible. The obtained simulation results are shown in Fig. 7.

It should be pronounced, that due to the proposed intelligent finite element, the relation between state variables (e.g. between stresses and strains) is already known before the finite element simulation starts and has not to be determined by iterative calculations of inelastic evolution processes during the simulations. This establishes the possibility to reduce computational costs and time. For this reason, the elastic material law is not replaced in the numerical simulations, because, in the present study, there is not any advantage regarding computational effort of an ANN compared to an elastic material law. The dependency in-between state variables in the elastic constitutive law is given by a matrix multiplication, equivalently to the proposed ANN for the viscoplastic model. The predicted curve using the intelligent finite element is presented versus the classical finite element simulation results and the measured mid-point deflections. As it can be observed, the correlation of the curve by means of the intelligent element, belonging to a peak pressure $pp = 3.5$ bar is much closer to the measurement as in Fig. 4. However, differences to the classical finite element method can be

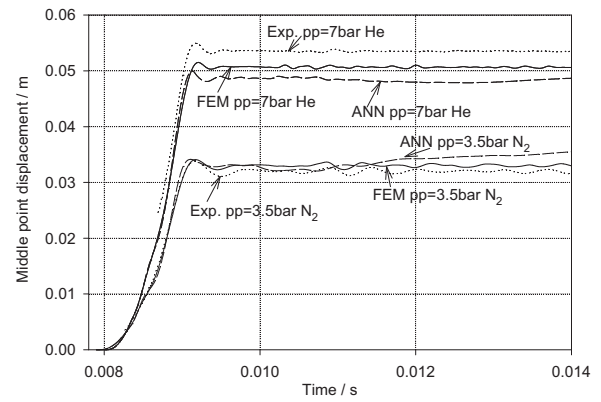


Fig. 7. Mid-point deflections using measurements, FEM and ANN simulations with intelligent elements.

found in Fig. 7. The analogous result is visible for a plate deflection with a peak pressure of $pp = 7$ bar. This could be explained by the interpolation of the ANN between given points in the trained data set. Due to the fact that the constitutive law is replaced by an ANN, the calculated result by means of a neural network can only tend towards the finite element result. However, the ANN simulation cannot predict the measurement better than the FEM result. The present example with the peak pressure $pp = 7$ bar can be improved by a higher density of input and output data for training the intelligent element. The more data points provided, the better the approximation of the ANN solution towards the FEM result. An interesting next step in developing intelligent finite elements would be to replace matrices in the system of the equations of motion in the finite element algorithm. These matrices, e.g. sum of internal forces, keep not only information about the constitutive law, but also relations of the structural behaviour inside. In this way, generalised force and displacement dependencies could be expressed by an ANN and not only stress strain relations.

The advantage of the intelligent element, used in the present study, is, that iteration processes with the constitutive law, as they are necessary in conventional finite element simulations, can be omitted in the ANN. Here, stresses, strains, strainrates, backstresses, and backstressrates are explicitly included in the training data. Therefore, the simulations by means of ANN led to the half of the computing time compared to the classical finite element method.

In Fig. 8 the stress evolutions in two points, where the maximum radial stresses in the plate occur, are shown for $pp = 7$ bar. In the plate centre at the bottom and at the boundary in the top of the plate, the stresses are plotted in the period when the structure is subjected to the shock-wave until the plate reaches its first amplitude.

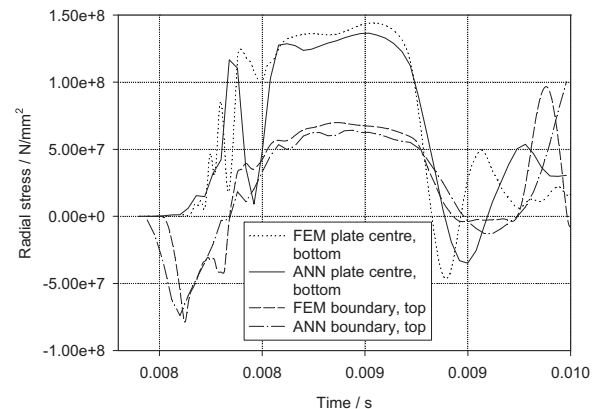


Fig. 8. Radial stress evolution using FEM and ANN simulations with intelligent elements.

In the cited previous studies, it was reported, that this time is essential for the shape forming of the structure due to the wave propagation within this period. The bottom of the plate is inside the shock tube, that means, it is subjected to the pressure wave. Even the appearance of stress waves is well predicted by the intelligent element, as it can be observed by the oscillating stress evolution in the plate centre. Due to the subjection of the plane pressure wave on the entire surface of the plate specimen, the wave propagation starts at the boundary, leading to oscillating stresses in the plate centre. The stress values are slightly different between the FEM and ANN method, however, e.g. the phase shift between two amplitudes of the FEM and ANN results is rather small with around one tenth of a millisecond. These differences in the stress distributions could be one indicator for the differences in Fig. 7, because the trained ANN has to interpolate, if the values for state variables do not occur exactly in the training data sets.

6. Discussion and conclusions

Two methods of developing ANNs have been proposed in the present study. In the first approach, experimental data was used only for the entire structural response. It was possible to train the neural network with these values, but the prediction of additional deformations outside of the trained data deviates from the measured mid-point deflections of the plate specimens. Consequently, the advantage of an ANN, to be very reliable since trained data is recalculated, was used to propose an intelligent finite element for viscoplastic material behaviour. However, it must be ensured that the occurring state variables in the intelligent finite element simulations are inside the provided set of constitutive training data. Following this method, simulation results being much more precise than in the first approach are obtained, but with considerably less computational effort than in classical finite element simulations. However, one intermediate step is necessary before the intelligent element is complete. The data set to train the ANN and to determine the synapse matrices have to be obtained numerically. In summary, the proposed method demonstrates the possibility to develop an ANN within an intelligent finite element for non-linear problems in structural mechanics. This method can be very efficient concerning the reliability of numerical predictions and can lead to a significant reduction of simulation time.

References

- [1] M. Shakiba, N. Parson, X.-G. Chen, Modeling the effects of cu content and deformation variables on the high-temperature flow behavior of dilute al-fe-si alloys using an artificial neural network, *Materials* 9 (536) (2016) 1–13.
- [2] A.-A. Chojaczyk, A.-P. Teixeira, C. Luis, J.-B. Cardoso, C.-G. Soares, Review and application of artificial neural networks models in reliability analysis of steel structures, *Struct. Saf.* 52 (A) (2015) 78–89.
- [3] G.-R. Liu, Y.-G. Xu, Z.-P. Wu, Total solution for structural mechanics problems, *Comput. Methods Appl. Mech. Eng.* 191 (2001) 989–1012.
- [4] Z. Waszczyszyn, L. Ziemiański, Neural networks in mechanics of structures and materials - new results and prospects of applications, *Comput. Struct.* 79 (2001) 2261–2276.
- [5] Z.-R. Tahir, P. Mandal, Artificial neural networks prediction of buckling load of thin cylindrical shells under axial compression, *Eng. Struct.* 152 (2017) 843–855.
- [6] J. Cheng, Q.-S. Li, Reliability analysis of structures using artificial neural network based genetic algorithms, *Comput. Methods Appl. Mech. Eng.* 197 (2008) 3742–3750.
- [7] D. Zhao, D. Ren, K. Zhao, S. Pan, X. Guo, Effect of welding parameters on tensile strength of ultrasonic spot welded joints of aluminum to steel - by experimentation and artificial neural network, *J. Manuf. Process.* 30 (2017) 63–74.
- [8] S. Mandal, P.-V. Sivaprasad, S. Venugopal, K.-P.-N. Murthy, Artificial neural network modeling to evaluate and predict the deformation behavior of stainless steel type aisi 304l during hot torsion, *Appl. Soft Comput.* 9 (2009) 237–244.
- [9] A.-A. Javadi, M. Rezaia, Applications of artificial intelligence and data mining techniques in soil modeling, *Geomech. Eng.* 1 (1) (2009) 53–74.
- [10] M. Shojaeefard, M. Akbari, M. Tahani, F. Farhani, Sensitivity analysis of the artificial neural network outputs in friction stir lap joining of aluminium to brass, *Adv. Mater. Sci. Eng.* 2013 (2013) 1–7 (ID 574914).
- [11] M. Lu, S.-M. AbouRizk, U.-H. Hermann, Sensitivity analysis of neural networks in spool fabrication productivity studies, *J. Comput. Civil. Eng.* 15 (4) (2001) 299–308.
- [12] R. Kaunda, New artificial neural networks for true triaxial stress state analysis and demonstration of intermediate principal stress effects on intact rock strength, *J. Rock. Mech. Geotech. Eng.* 6 (2014) 338–347.
- [13] A.-A. Javadi, M. Mehravar, A. Faramarzi, A. Ahangar-Asr, An artificial intelligence based finite element method, *ISAST Trans. Comput. Intell. Syst.* 1 (2) (2009) 1–7.
- [14] V. Papadopoulos, G. Soimiris, D.-G. Giovanis, M. Papadarakakis, A neural network-based surrogate model for carbon nanotubes with geometric nonlinearities, *Comput. Methods Appl. Mech. Eng.* 328 (2018) 411–430.
- [15] M. Lefik, D.-P. Boso, B.-A. Schrefler, Artificial neural networks in numerical modeling of composites, *Comput. Methods Appl. Mech. Eng.* 198 (2009) 1785–1804.
- [16] H. Shin, G. Pande, On self-learning finite element code based on monitored response of structures, *Comput. Geotech.* 27 (3) (2000) 161–178.
- [17] A.-A. Javadi, M. Rezaia, Intelligent finite element method: an evolutionary approach to constitutive modeling, *Adv. Eng. Inform.* 23 (2009) 442–451.
- [18] F. Salvado, F. Teixeira-Dias, S. Walley, L. Lea, J. Cardoso, A review on the strain rate dependency of the dynamic viscoplastic response of fcc metals, *Progress. Mater. Sci.* 88 (2017) 186–231.
- [19] F. Covezzi, S. de Miranda, S. Marfia, E. Sacco, Homogenization of elastic-viscoplastic composites by the mixed tfa, *Comput. Methods Appl. Mech. Eng.* 318 (2017) 701–723.
- [20] T.-A. Bui, H. Wong, F. Deleruyelle, L.-Z. Xie, D.-T. Tran, A thermodynamically consistent model accounting for viscoplastic creep and anisotropic damage in unsaturated rocks, *Int. J. Solids Struct.* 117 (2017) 26–38.
- [21] M. Stoffel, Evolution of plastic zones in dynamically loaded plates using different elastic-viscoplastic laws, *Int. J. Solids Struct.* 41 (2004) 6813–6830.
- [22] V.-K. Ojha, A. Abraham, V. Šnášel, Metaheuristic design of feedforward neural networks: a review of two decades of research, *Eng. Appl. Artif. Intell.* 60 (2017) 97–116.
- [23] Z. Lu, X. Pan, Q. Liu, Y. Qin, Y. He, S. Cao, Artificial neural network prediction to the hot compressive deformation behavior of al-cu-mg-ag heat-resistant aluminium alloy, *Mech. Res. Commun.* 38 (2011) 192–197.
- [24] N. Kiliç, E. Bülent, S. Hartomacioğlu, Determination of penetration depth at high velocity impact using finite element method and artificial neural network tools, *Def. Technol.* 11 (2015) 110–122.
- [25] A. Engelbrecht, *Computational Intelligence, An Introduction*, John Wiley & Sons, The Atrium, Southern Gate, Chichester, West Sussex PO19 8SQ, England, 2007.
- [26] A. Ajmani, D. Kamthania, M.-N. Hoda, A comparative study on constructive and non-constructive supervised learning algorithms for artificial neural networks, in: *Proceedings of the 2nd National Conference, Bharati Vidyapeeth's Institute of Computer Applications and Management, New Delhi, INDIACom - 2008*.
- [27] J. Lemaitre, J. Chaboche, *Mechanics of Solid Materials*, Cambridge University Press, The Edinburgh Building, Cambridge CB2 8RU, UK, 1994.